



Using a two-stage Rosenbrock solver to improve surface ozone prediction and increase computational efficiency in the DOE's Exascale Earth System Model version 1 (E3SMv1)

Rong-You Chien¹, Joshua S. Fu^{1,2*}

5 ¹Department of Civil and Environmental Engineering, University of Tennessee, Knoxville, Tennessee, USA

²Integrated Computational Earth Sciences Group, Oak Ridge National Laboratory, Oak Ridge, Tennessee, USA

Correspondence to: J. S. Fu (jsfu@utk.edu)

Abstract. The integration of stiff atmospheric chemical systems is a major computational cost in Earth System Models and poses challenges for numerical stability and scalability as chemical complexity and temporal resolution increase. Current
10 implementations commonly rely on fully implicit Newton–Raphson-based solvers, which are robust but computationally expensive. In this study, we implement a semi-implicit two-stage Rosenbrock method (ROS2) in the Energy Exascale Earth System Model version 1 (E3SMv1) and evaluate its performance as an alternative chemistry time-integration scheme. The ROS2 solver is applied to two interactive chemical mechanisms of differing stiffness and size: chemUCI (60 prognostic species) and trop_strat_mozart_mam4 (155 prognostic species). Numerical experiments include short simulations to quantify
15 computational cost and year-long integrations to assess numerical stability, solution consistency, and long-term behavior. Solver performance is evaluated under identical model configurations and timesteps. At a 180-second timestep, ROS2 reduces chemistry integration cost by approximately 33% relative to the default implicit solver. Differences in global mean surface ozone concentrations are small (≤ 1.03 ppb), and no systematic drift or degradation in numerical stability is observed over one-year simulations. These results indicate that low-order Rosenbrock methods provide a computationally efficient and
20 numerically stable alternative for stiff atmospheric chemistry integration in E3SMv1. The implementation offers a flexible framework for future model configurations with increased chemical complexity and resolution.



1 Introduction

Tropospheric ozone is one of the major air pollutants that has been monitored for decades due to its adverse impacts on human health, ecosystems, and agricultural productivity. Ground-level ozone can trigger respiratory disease, penetrate leaves, and reduce crop yields; therefore, it must be monitored and predicted as both an air pollutant and a climate-relevant species (Markandya et al., 2018; Vandyck et al., 2018). Accurate simulation of surface ozone remains a core capability of numerical models used for air-quality assessment and Earth-system prediction. In the United States, the US EPA has regulated tropospheric ozone under the National Ambient Air Quality Standards (NAAQS) since 1971. NAAQS standards have supported monitoring of many chemical species and evaluation of regulatory controls on precursor emissions (e.g., ozone, carbon monoxide, and NO_x). Long-lived species such as ozone have lifetimes spanning weeks to months in the troposphere and will remain relevant through mid-century in future scenarios assessed by the IPCC AR6 (Szopa et al., 2023). In contrast, short-lived species such as NO_x can act as precursors to multiple pollutants (Brasseur et al., 1999), contributing to strong spatial heterogeneity. Because atmospheric chemistry couples species spanning from seconds to months, robust and efficient simulation of such systems remains a major challenge.

To better represent production and loss processes, interactive atmospheric chemistry has increasingly been incorporated into chemistry–climate mechanisms since the 1980s (Cariolle and Déqué, 1986; Cariolle and Teysseire, 2007). Compared with prescribed-chemistry approaches, interactive chemistry allows reaction rates and chemical pathways to respond dynamically to meteorological conditions (e.g., temperature and radiation), thereby improving internal consistency. Despite these advantages, many Global Climate Models (GCMs) and Earth System Models (ESMs) still rely on prescribed chemistry fields to reduce computational cost (Hurrell et al., 2013). These prescribed concentrations may be derived from observationally constrained products or from other gridded model simulations. However, not every chemical species is consistently available at the global scale across applications and intercomparisons. For example, only 8 of 23 CMIP3 models included black carbon, and fewer than half included future changes in tropospheric ozone (Lamarque et al., 2013). Other chemically important species, such as isoprene—potentially a significant contributor to secondary organic aerosol (SOA) are often excluded for computational efficiency. As a result, GCMs and ESMs may rely on multiple sources of chemical concentration fields, for instance, ozone (Cionni et al., 2011), greenhouse gases (Meinshausen et al., 2011), and anthropogenic and biomass-burning emissions (Lamarque et al., 2010) for CESM1, all coming from different sources. While computationally efficient, combining prescribed fields from different sources can introduce inconsistencies when chemical processes are decoupled from evolving meteorological states, especially as model resolution increases and chemical complexity grows.

Although prescribed chemistry can reduce computational cost in global-scale simulations, inconsistent chemistry may compromise internal numerical consistency and lead to biases. For example, ozone production and loss depend on reactive oxygen chemistry, and reaction rates depend strongly on temperature; warming associated with climate change can therefore alter reaction rates relative to those implicit in prescribed concentration fields. This motivates the use of dynamical chemistry solvers that directly couple reaction rates and chemical evolution to the simulated meteorology.



Using a dynamical chemistry solver in an ESM helps maintain numerical consistency between chemical reaction rates and meteorological conditions. Some models, such as WACCM, use simplified gas-phase chemistry (Neale et al., 2012). Other models include interactive chemistry through additional coupled modules, such as LMDZ-INCA (Hauglustaine et al., 2004), in part because of the enormous computational cost associated with solving complex chemical reactions. Yet many GCMs and
60 ESMs aiming to represent more realistic biogeochemical cycles require more complex ozone and tracer chemistry. Examples include linearized ozone chemistry used in stratospheric ozone modeling (McInden et al., 2000), the tropospheric model for ozone and related chemical tracers (trop_MOZART) (Emmons et al., 2010), and the more extensive tropospheric-and-stratospheric MOZART (trop_strat_mozart) (Lamarque et al., 2012), which has been used in ESMs such as the Community Atmosphere Model (CAM) within CESM (Neale et al., 2012; Tilmes et al., 2015). However, integrating stiff ODE systems is
65 a major computational bottleneck when simulating species with lifetimes ranging from seconds and minutes to more than one day.

The efficiency of numerical solvers for chemistry interactions is therefore a critical issue (Brasseur et al., 1999; Santillana et al., 2010; Sun et al., 2017). A key difficulty is integrating species spanning a wide range of lifetimes. Models adopt different strategies to address stiffness and timescale separation. For example, the fully coupled model WACCM used an explicit method
70 for long-lived species with weak forcing terms and a fixed 30-minute-timestep Newton–Raphson iteration for short-lived species (Neale et al., 2012). Iterative implicit solvers can provide stable integration but may be limited by large timesteps when species lifetimes are minutes or seconds (e.g., during rapid ozone formation). Reducing timesteps can improve fidelity but may increase the number of iteration counts and total computational cost, motivating the development and implementation of more efficient solvers.

Sandu et al. (1997b) compared several implicit solvers, including the Livermore Solver for Ordinary Differential Equations (LSODE), Variable coefficient Ordinary Differential Equation (VODE), Singly Diagonally Implicit Runge–Kutta (SDIRK4), and the Rosenbrock solver RODAS. They concluded that sparse RODAS is more efficient in most test cases. Verwer et al. (1999) further developed a stable second-order two-stage Rosenbrock method (ROS2), suitable for large timesteps on mechanisms such as RIVM, CBM-IV, and WET. Sun et al. (2017) implemented ROS2 in the Community Earth System Model
80 (CESM) and found that, at the same timestep, ROS2 reduced the computational cost by 47% relative to the original numerical scheme.

This paper evaluates ROS2 within the Energy Exascale Earth System Model version 1 (E3SMv1), which is designed to support high-resolution, process-rich Earth system simulations on next-generation computing architectures. The atmosphere component (E3SM Atmosphere Model, EAM) is branched from CAM5 and adopts a spectral-element dynamical core that
85 supports variable-resolution regional refinement and enhanced vertical resolution (Golaz et al., 2019; Leung et al., 2020). Although Rosenbrock solvers have been evaluated in other finite-difference-core ESMs, their implementation and performance within the finite-element-core E3SMv1 have not been systematically assessed. We test ROS2 using two chemistry mechanisms adapted for E3SMv1: the MOZART4 mechanism (Emmons et al., 2010; Tilmes et al., 2015) and the UC Irvine chemistry-transport model (chemUCI) (Prather et al., 2017; Tang and Prather, 2012). While both mechanisms can produce ozone



90 concentrations, the objective here is not to compare their chemical outcomes; rather, they provide complementary testbeds to assess implementation robustness and solver performance across different chemical stiffness and complexity.

We examine three numerical scenarios for both chemical mechanisms to evaluate the performance of ROS2 as implemented in E3SMv1. The first experiment consists of a one-day simulation with two different CPU configurations to assess computational efficiency. The second experiment involves a one-year simulation designed to evaluate temporal behavior, 95 numerical consistency, and the range of simulated chemical concentrations across solver configurations. The one-year simulation used branches from the E3SMv1, which has been archived in (Tang et al., 2026), and the output can be found in Chien and Fu (2026d) and Chien and Fu (2026c). Together, these experiments provide a comprehensive assessment of solver efficiency and short-to-intermediate numerical stability relevant to operational Earth System Model applications and directly support the broader ESM community by enabling more scalable chemistry–climate coupling in a next-generation, variable- 100 resolution model framework.

These advances are particularly timely given emerging CMIP7 and exascale Earth system modeling priorities. CMIP7 emphasizes higher spatial resolution, more comprehensive Earth system coupling, and improved representation of short-lived climate forcers, including tropospheric ozone and its precursors, while maintaining feasibility on next-generation computing architectures (Dunne et al., 2025; Mcpartland et al., 2025; Szopa et al., 2023). Achieving these goals requires numerical 105 methods that are not only physically consistent but also computationally scalable across massively parallel systems. Chemistry solvers capable of efficiently handling stiff, multiscale reaction systems are, therefore, a critical enabling technology for CMIP7-class simulations, especially as ESMs transition toward variable-resolution grids, regionally refined domains, and increasingly complex atmospheric chemistry. Improving solver efficiency directly supports the CMIP7 objective of expanding process fidelity without prohibitive increases in computational cost.

110 **2 Model and Method Used**

This study employs the Energy Exascale Earth System Model version 1 (E3SMv1), which was developed to support high-resolution, process-rich Earth system simulations on current and emerging high-performance computing architectures (Golaz et al., 2019). E3SMv1 is designed to address modeling priorities relevant to next-generation CMIP-class simulations, including scalable numerical performance, variable-resolution grids, and enhanced representation of atmospheric processes (Leung et 115 al., 2020). The atmospheric component of E3SMv1, the E3SM Atmosphere Model (EAM), is branched from the Community Atmosphere Model version 5 (CAM5) (Neale et al., 2012) and employs a spectral-element dynamical core. This finite-element formulation enables high-order accuracy, efficient parallel scalability, and regional mesh refinement within a global framework, distinguishing E3SM from many previous chemistry–climate models that rely on finite-difference dynamical cores.

120 Interactive atmospheric chemistry is used to simulate the production, transformation, and loss of ozone and related chemical tracers. Two chemistry mechanisms adapted for use within E3SMv1 are employed in this study. The first is MOZART4, a



comprehensive tropospheric chemistry mechanism that represents ozone–NO_x–VOC interactions and has been widely used in Earth System Models, including CESM (Emmons et al., 2010; Lamarque et al., 2012; Tilmes et al., 2015; Neale et al., 2012). The second is chemUCI, the UC Irvine chemistry-transport model, which emphasizes tropospheric ozone chemistry and provides an alternative formulation of chemical reaction pathways (Prather et al., 2017; Tang and Prather, 2012). In both cases, chemistry is solved interactively within EAM and fully coupled to meteorological fields, allowing reaction rates to respond dynamically to temperature, radiation, and transport processes, consistent with earlier developments in interactive chemistry–climate modeling. The two mechanisms are not compared in terms of chemical outcomes; rather, they serve as complementary test cases to evaluate numerical solver performance across varying levels of chemical complexity and stiffness.

125 Atmospheric chemistry is represented mathematically as a system of stiff ordinary differential equations (ODEs) describing gas-phase chemical reactions with characteristic timescales ranging from seconds to months (Brasseur et al., 1999). In the default E3SMv1 configuration, these equations are integrated using an iterative implicit solver with a fixed chemistry time step, similar to approaches employed in other fully coupled chemistry–climate models such as WACCM. In this study, the second-order Rosenbrock solver (ROS2) is implemented as an alternative chemistry integration method (Verwer et al., 1999).

130 ROS2 is a linearly implicit solver designed for stiff ODE systems and provides second-order temporal accuracy while avoiding costly nonlinear iterations. Previous studies have demonstrated that Rosenbrock-type solvers are efficient and stable for atmospheric chemistry applications (Santillana et al., 2010; Sandu et al., 1997a), and ROS2 has been shown to substantially reduce computational cost when implemented in CESM relative to traditional numerical schemes (Sun et al., 2017).

The ROS2 solver is integrated into the existing E3SMv1 chemistry framework without modification to chemical reaction mechanisms, species definitions, or transport formulations. This design ensures that any differences observed between simulations arise solely from the numerical integration method, rather than from changes in chemical physics or parameterizations. The solver implementation is therefore directly relevant to Earth System Model development, particularly for CMIP7-era simulations that require scalable, numerically robust chemistry solvers capable of supporting higher spatial resolution, increased chemical complexity, and execution on exascale computing architectures.

140 A series of numerical experiments is conducted to evaluate the performance of the ROS2 solver within E3SMv1. Short-term simulations of one day are performed using different CPU configurations to quantify computational efficiency and chemistry-related computational cost. Longer one-year simulations are used to assess numerical stability, temporal behavior, and the range of simulated chemical concentrations over climate-relevant timescales. Additional sensitivity experiments examine solver behavior under different chemistry time-step configurations. All simulations use identical initial conditions, emissions, boundary conditions, and physical parameterizations to isolate the impact of the chemistry solver.

145 Solver performance is evaluated using metrics commonly applied in chemistry–climate model development studies, including total wall-clock time, chemistry-related CPU cost, numerical stability, and temporal consistency of key chemical species (Brasseur et al., 1999; Santillana et al., 2010; Sun et al., 2017). These metrics directly address the requirements of scalable and internally consistent chemistry–climate coupling in next-generation Earth system models and support the broader modeling community by enabling more efficient integration of interactive chemistry into CMIP-class and exascale simulations.

155



The chemical species for each grid in the interactive chemistry mechanism of the E3SMv1 have the equation form, which can be presented as,

$$\frac{Dy}{Dt} = F(y) = P(y) - L(y) + I(y) \quad (1)$$

where $y = (y_1, y_2, \dots, y_N)^T$ is the vector of volume mixing ratios for N species. The source term $F(y)$ can be further decomposed into three terms: the production for these chemical species $P(y)$, the losing term for the consumption of these chemical species $L(y)$, and $I(y)$ the independent forcing term, which is based on the external forcing. To solve the set of time-dependent ordinary differential equations, a matrix form of the chemical equations is established (Fig. 1). The Newton-Raphson iteration has been adopted as the numerical solver in some global climate models, such as CESM (Neale et al., 2012). This iteration solver benefits from its long timestep and can use the same timestep as the atmospheric component. However, using a long timestep may limit the reaction's performance with shorter-lived chemical species. This limitation would result in the use of parameters for these chemical components. Rosenbrock (1963) proposed generalizing the linearly implicit approach by using multiple stages to achieve higher-order consistency. In this paper (Chien and Fu, 2026b), we proposed a two-stage Rosenbrock scheme. The two-stage Rosenbrock scheme (ROS2) is a well-known numerical scheme for solving stiff Ordinary Differential Equations (stiff ODEs). The solution of the ODE equation can be achieved by rewriting the equation as

$$(I - h\gamma A)k_1 = F(y^n) \quad (2)$$

$$(I - h\gamma A)k_2 = F(y^n + hk_1) - 2k_1 \quad (3)$$

$$y^{n+1} = y^n + \frac{3}{2}hk_1 + \frac{1}{2}hk_2 \quad (4)$$

where I is $N \times N$ identity matrix, h is the timestep and $A = \frac{\partial F(y)}{\partial y} \Big|_{y=y^n}$ is the Jacobian matrix at time $t = t^n$. y^n and y^{n+1} are the solution vectors at time $t = t^n$ and $t = t^{n+1}$, respectively. The vectors k_1 and k_2 are the intermediate solutions at each stage. The parameter γ is used in the stability function,

$$R(z) = \frac{1 + (1 - 2\gamma)z + \left(\frac{1}{2} - 2\gamma + \gamma^2\right)z^2}{(1 - \gamma z)^2} \quad (5)$$

This stability function $R(z)$ is A-stable if and only if $\gamma \geq \frac{1}{4}$. Furthermore, to have L-stable $R(\infty) = 0$, which can fulfill the radical chemistry species with a short life span, the parameter should be chosen as $\gamma = 1 \pm \frac{\sqrt{2}}{2}$ (Verwer et al., 1999). Here, we set $\gamma = 1 + \frac{\sqrt{2}}{2}$. Previous research has demonstrated that the ROS2 solver can support chemistry timesteps of approximately 10–20 minutes for complex chemical mechanisms (Sandu et al., 1997b; Verwer et al., 1999). These studies primarily focused on solver performance in idealized or offline chemical modeling frameworks and emphasized timestep stability rather than solver behavior within fully coupled Earth system models. In such coupled systems, additional constraints arise from interactions with transport, vertical diffusion, and physics parameterizations, which can significantly limit the practical timestep. Sun et al. (2017) showed that, when ROS2 was implemented in the Community Earth System Model (CESM), a



180 much shorter chemistry timestep of approximately 3 minutes was required under operational model configurations. While adopting a shorter timestep can yield more realistic simulations of fast chemical reactions compared to traditional Newton–Raphson iteration schemes, it also increases computational demands, particularly for high-resolution and chemistry-rich simulations.

The present study advances beyond these earlier investigations by evaluating ROS2 within a fully coupled, variable-resolution Earth System Model designed for exascale computing, rather than focusing solely on achievable timestep lengths. By embedding ROS2 in E3SMv1, which employs a finite-element dynamical core and supports regional refinement, this work assesses solver performance under numerical and coupling constraints that are representative of next-generation operational Earth System Models. This approach extends previous solver-focused studies by explicitly examining numerical consistency, computational efficiency, and parallel scalability in a framework aligned with emerging CMIP7 and exascale modeling priorities.

The experimental design emphasizes solver behavior under production-relevant configurations rather than idealized test cases. A series of one-day simulations is performed for each solver configuration, using two different CPU core counts, to quantify the chemistry-related computational cost and parallel performance. To evaluate numerical consistency and temporal behavior beyond short-term metrics, one-year simulations are conducted to examine global mean concentrations and diurnal cycles of key chemical species. These simulation durations are sufficient to assess solver efficiency and short-to-intermediate numerical stability in stiff atmospheric chemistry systems, while deliberately avoiding analysis of long-term climate variability or observational comparisons, consistent with the methodological scope of Geoscientific Model Development.

All simulations are conducted on the Cray XC-based Cori supercomputer at the National Energy Research Scientific Computing Center (NERSC) (Doerfler et al., 2018), using Intel Knights Landing (KNL) processors in stand-alone mode. Each KNL node contains 68 cores. A baseline configuration with 693 cores is used for general solver testing, while a higher-core configuration with 1350 cores is used to assess performance and scalability across all experimental scenarios. This computing environment enables direct evaluation of solver behavior on leadership-class architectures representative of current and future Earth system modeling platforms.

3 Results and Discussion

205 For a numerically consistent time-integration scheme, the truncation error, ϵ , is expected to scale with a power of the timestep or grid spacing (Ferziger and Perić, 2002; Moin, 2010) and can be expressed as $\epsilon = o(\Delta t^k)$ where k denotes the formal order of accuracy. While such theoretical convergence behavior is well established for idealized systems, its realization in atmospheric chemistry solvers remains uncertain under realistic reaction rates, stiffness, and coupling constraints typical of Earth System Models. Assessing solver accuracy under operational chemical conditions is therefore essential for understanding numerical behavior beyond idealized test problems. To directly evaluate solver accuracy and stability under realistic chemical kinetics, we develop a box-model framework (Chien and Fu, 2026a) that uses actual chemical reaction rates and species



interactions extracted from the full Earth System Model (the extracted dataset can be found in Chien and Fu (2026e)). This approach enables controlled numerical testing while retaining the stiffness, sparsity, and multiscale characteristics of operational atmospheric chemistry. The box model is used to compare the original implicit solver (IMP) with the two-stage
215 Rosenbrock solver (ROS2), allowing a direct assessment of numerical behavior without confounding effects from transport or physics parameterizations. The box model is constructed using chemical interaction data from the first simulation day, comprising 49 chemistry timesteps, as used in both chemUCI and trop_strat_mozart_mam4 configurations. The dataset includes 48,602 atmospheric columns, each with 72 vertical layers, representing a wide range of chemical environments and stiffness regimes encountered in the full model. These data are used to assemble the sparse Jacobian matrix shown in Figure
220 1, which faithfully reflects the structure and complexity of chemistry operators in a fully coupled Earth System Model. This methodology advances beyond traditional solver assessments that rely on simplified or synthetic chemical systems. By grounding the numerical analysis in real, model-generated chemistry, the box-model framework bridges theoretical numerical analysis and operational Earth system modeling. It provides a robust basis for evaluating solver accuracy, stability, and scalability in a manner directly relevant to next-generation, chemistry-rich, Exascale Earth system simulations. For truncation
225 error $\epsilon_i = y - y_i$, where y is the analytical solution, and y_i the numerical error. Since we do not know the analytical solution y , when Δt_1 is larger than Δt_2 , we can have:

$$|\epsilon_1 - \epsilon_2| = |y_1 - y_2| = |o(\Delta t_1^k) - o(\Delta t_2^k)| \approx |o(\Delta t_1^k)| = a(\Delta t_1^k) \quad (6)$$

where k is the order of accuracy and ϵ_1 and ϵ_2 are the truncational error based on the timestep Δt_1 and Δt_2 . Thus, the error estimation can be expressed as

$$\log_{10}|y_1 - y_2| = \log_{10} a + k(\log_{10} \Delta t_1) \quad (7)$$

and the slope of the log-log plot for the timestep and results difference can be used as a measurement of the order of accuracy.
230 To quantify numerical accuracy under realistic chemical conditions, a box-model framework was used to estimate the truncation error, ϵ_i , for each solver. The box model employs actual chemical reaction rates and mixing ratios extracted from the full Earth system model, thereby retaining the stiffness and multiscale behavior of operational atmospheric chemistry. For both the Newton–Raphson implicit solver and the two-stage Rosenbrock solver, the timestep is successively halved at each iteration, starting from 1800s (denoted IMP_1800 and ROS2_1800, respectively). This approach enables estimation of the
235 solver's convergence behavior under realistic chemical kinetics rather than on idealized test problems. Figure 2 summarizes the convergence results for both chemistry mechanisms. Results are shown for one representative grid column (solid lines) as well as the mean slope (dashed lines) computed across 10,000 randomly sampled grid columns, spanning all vertical levels and timesteps from the first simulation day after 25 iterations. Results are presented for chemUCI (Fig. 2a) and trop_strat_mozart_mam4 (Fig. 2b), with the implicit solver shown in blue and the two-stage Rosenbrock shown in red. In both
240 mechanisms, the ROS2 solver exhibits faster convergence than the original implicit solver. For chemUCI, the mean slope is -0.34 for IMP and -0.68 for ROS2, while for trop_strat_mozart_mam4, the mean slopes are -0.30 and -0.50 , respectively. These results are consistent with the theoretical expectation that the iterative implicit solver is first-order accurate, whereas the two-stage Rosenbrock solver approaches second-order accuracy under realistic reaction-rate conditions. Importantly, this



convergence behavior is demonstrated using real chemistry extracted from a fully coupled Earth System Model, providing
245 stronger evidence of solver robustness than prior idealized studies.

Although the box-model experiments indicate that the timestep of 1800s is numerically feasible, accumulated numerical errors
in a fully coupled climate model may still compromise long-term stability. Consequently, a shorter timestep is required for
operational Earth system simulations. Verwer et al. (1999) suggested ROS2 timesteps of 600–1200s for chemistry models such
as RIVM, CBM-IV, and WET. However, due to the finer vertical resolution and stronger coupling constraints in Earth System
250 Models, Sun et al. (2017) recommended a chemistry timestep of 180s for ROS2 in CESM. Following this guidance, we adopt
a 180s timestep for ROS2 in E3SM, denoted ROS2_180. Two additional numerical configurations are defined for comparison:
the original implicit solver with a timestep of 1800s (IMP_1800, reference run) and the implicit solver with a timestep of 180s
(IMP_180, intermediate run). All three configurations use identical reaction rates and matrix mappings, isolating the effects
of solver formulation and timestep selection.

255 The computational cost of each numerical configuration is evaluated using one-day simulations on 693 and 1350 CPU cores
(Fig. 3). For trop_strat_mozart_mam4 (Fig. 3a), ROS2_180 requires only 67.64% of the computational time of IMP_180 using
693 cores and 67.20% using 1350 cores. Similar results are obtained for chemUCI (Fig. 3b), where ROS2_180 uses 67.38%
and 67.66% of the IMP_180 runtime at 693 and 1350 cores, respectively. These results demonstrate that ROS2 is
approximately 33 % more efficient than the original implicit solver at the same timestep. While reducing the timestep in the
260 implicit solver also improves stability, Neale et al. (2012) noted that failed convergence at longer timesteps can lead to repeated
iterations within the same grid cell, increasing computational cost. This behavior explains why the runtime of IMP_1800
exceeds one-tenth that of IMP_180, despite a tenfold difference in the timestep.

To assess solver behavior over climate-relevant timescales, one-year simulations are performed for all numerical
configurations. Figure 4 presents daily mean global surface ozone anomalies relative to IMP_1800 for chemUCI (Fig. 4a) and
265 trop_strat_mozart_mam4 (Fig. 4b). In chemUCI, ROS2_180 closely follows the temporal evolution of IMP_1800, with a small
mean difference of 0.11 ppb. In trop_strat_mozart_mam4, ROS2_180 also captures the overall temporal variability but
produces slightly lower surface ozone, with a mean difference of 1.03 ppb. These differences are small relative to typical
model variability and indicate that the new solver does not introduce spurious temporal behavior.

Spatial differences between ROS2_180 and IMP_1800 are shown in Figure 5. For chemUCI (Fig. 5a), global differences are
270 generally small, with slightly higher surface ozone in the Northern Hemisphere and localized differences near the Indian coast.
For trop_strat_mozart_mam4 (Fig. 5b), ROS2_180 yields lower surface ozone globally, with the largest reductions over North
Africa. The spatial patterns differ between mechanisms, indicating that ROS2 does not introduce a systematic bias toward
either higher or lower ozone concentrations.

The temporal consistency of solver behavior is further illustrated by the global diurnal cycles of surface ozone (Fig. 6). In
275 chemUCI (Fig. 6a), ROS2_180 produces a slightly higher mean ozone concentration than IMP_1800 (0.11 ppb), while in
trop_strat_mozart_mam4 (Fig. 6b), ROS2_180 yields a slightly lower mean (1.03 ppb). In both cases, the amplitude, phase,



and variability of the diurnal cycle are nearly identical across solvers, indicating that ROS2 preserves key temporal characteristics while improving numerical efficiency.

280 Diurnal cycles of additional chemical species are shown in Fig. 7. Because tropospheric ozone has a relatively long lifetime of approximately 10–40 days (Prather and Zhu, 2024), its diurnal variability is inherently smooth for models using minute-scale timesteps. For short-lived species such as OH (lifetime < 1 s) and moderately reactive species, all three numerical configurations produce nearly identical diurnal cycles in both chemistry mechanisms. For longer-lived species such as NO and NO₂, larger differences are observed between IMP_1800 and ROS2_180; however, comparisons with IMP_180 indicate that these differences arise primarily from timestep selection rather than solver formulation. This result demonstrates that the choice
285 of timestep exerts a stronger influence than the solver type on diurnal behavior for long-lived species.

Overall, these results show that the two-stage Rosenbrock solver provides substantially improved computational efficiency, maintains numerical stability, and preserves the realistic temporal and spatial behavior of key chemical species. By demonstrating robust solver performance within a fully coupled, variable-resolution Earth System Model, this study provides strong evidence that ROS2 is well-suited for next-generation, chemistry-rich, exascale Earth system simulations.

290 **4 Conclusion**

Tropospheric ozone is both a major air pollutant and an important greenhouse gas that absorbs solar radiation and contributes to warming in the lower atmosphere. Despite its central role in air quality and climate, fewer than half of CMIP-class Earth System Models explicitly simulate future changes in tropospheric ozone, primarily due to the high computational cost of interactive atmospheric chemistry. Addressing this limitation is essential for next-generation climate projections, particularly
295 as Earth System Models move toward higher spatial resolution, more complex chemistry, and stronger coupling across components.

In this study, we demonstrate that a high-efficiency chemistry solver traditionally used in regional air quality models can be successfully adapted for global Earth System Modeling. We implemented the two-stage Rosenbrock (ROS2) semi-implicit solver, previously applied in regional models such as CMAQ, within the global Earth System Model E3SMv1 and evaluated
300 its performance against the default Newton–Raphson iteration scheme. Across two chemically distinct mechanisms, ROS2 achieved approximately 33 % higher computational efficiency than the original implicit solver at the same fine temporal resolution. This result establishes, for the first time, that Rosenbrock-type solvers can deliver substantial performance gains in a fully coupled, variable-resolution, global Earth System Model.

305 While the stability of the ROS2 solver requires the use of a shorter timestep in global simulations, its increased efficiency provides a practical and scalable pathway to maintain interactive chemistry as models transition to finer spatial and temporal resolutions. This capability is particularly important for Earth System Models that dynamically shorten timesteps in response to enhanced vertical resolution or regional refinement. Our results show that solver choice, rather than timestep length alone, plays a critical role in enabling efficient chemistry–climate coupling under these conditions.



310 Model evaluation demonstrates that replacing the original implicit solver with ROS2 preserves the integrity of simulated chemical fields. Global diurnal cycles, spatial distributions, and temporal variability of surface ozone remain highly consistent across solvers, with differences in the global mean surface ozone below 1.03 ppb. Importantly, differences in diurnal behavior are shown to arise primarily from timestep selection rather than from the numerical solver itself. These findings confirm that the ROS2 solver improves computational efficiency without introducing systematic numerical bias or degrading chemical realism.

315 Beyond immediate performance gains, this work provides a foundational advance for future Earth System Modeling. The semi-implicit Rosenbrock framework offers increased flexibility for incorporating additional chemical species, representing fast-reacting processes, and harmonizing global and regional chemistry treatments within a unified modeling system. By enabling efficient interactive chemistry under increasingly demanding model configurations, this approach directly supports emerging priorities for CMIP7 and exascale Earth system simulations, where process fidelity, scalability, and computational
320 feasibility must advance together.

Overall, this study demonstrates that adopting advanced numerical solvers rather than simplifying chemistry offers a viable and forward-looking strategy for expanding chemical complexity in global Earth System Models. The implementation and evaluation of the ROS2 solver in E3SMv1 provide a clear pathway toward more comprehensive, efficient, and physically consistent simulations of tropospheric ozone and other chemically active species in next-generation climate models.

325



Figures

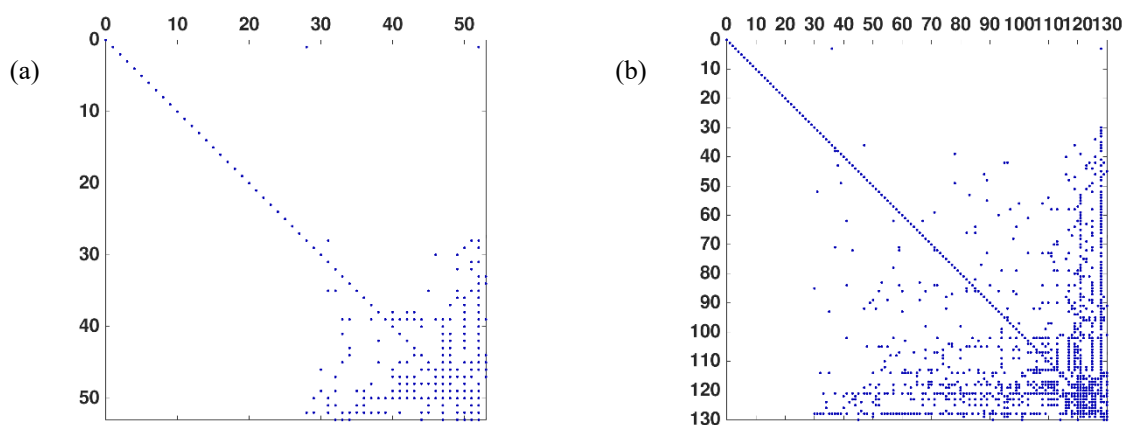


Figure 1. The non-zero element matrix pattern for (a) chemUCI, and (b) trop_strat_mozart_mam4. The blue spot indicates the location of the non-zero chemical species, which involves the reactions within this row and column.

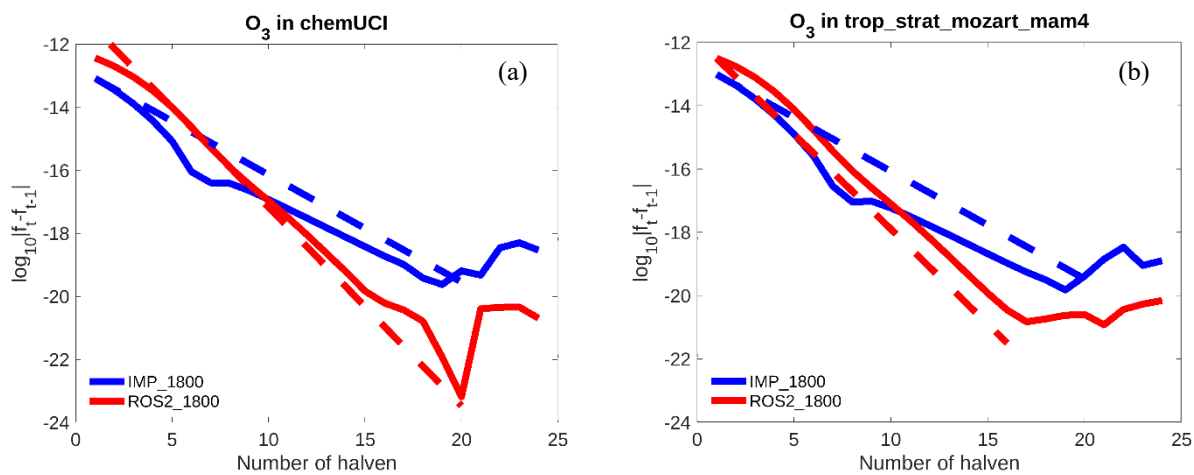


Figure 2. The convergence rate for one grid (solid lines), and the mean convergence rate for the 10,000 random grids (dashed lines) in both (a) chemUCI and (b) trop_strat_mozart_mam4. Blue lines are results for the implicit solver with timestep starting from 1800s (IMP_1800), and the red lines are for the Rosenbrock solver with timestep starting from 1800s (ROS2_1800).

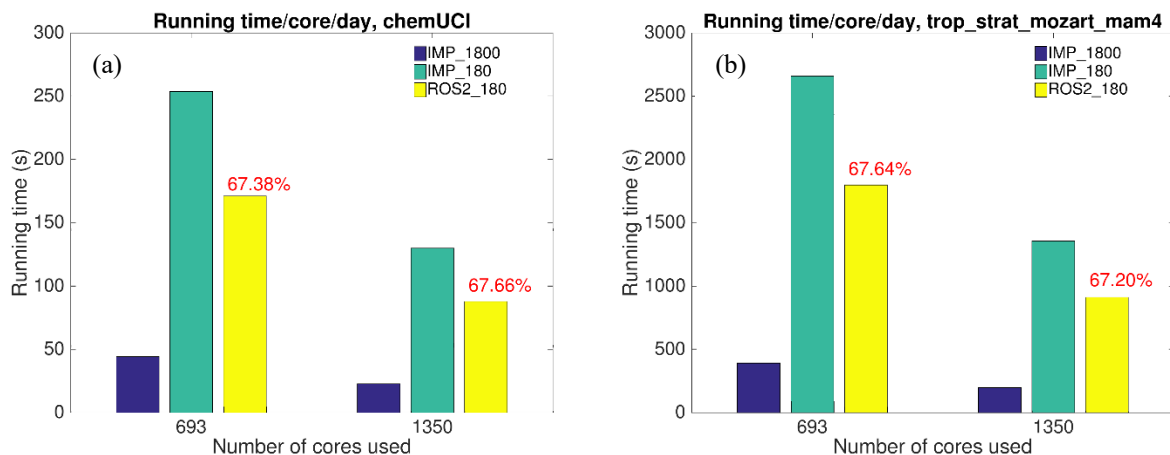


Figure 3. The running time for (a) chemUCI and (b) trop_strat_mozart_mam4. The dark blue is the iterative implicit solver with 1800s timestep (IMP_1800), and light green is IMP_180, and the yellow is the semi-implicit two-stage Rosenbrock solver with 180s timestep (ROS2_180) under 693 cores and 1350 cores. The efficiency of ROS2, expressed as a percentage, is shown

340 for each number of cores and chemistry mechanism in red.

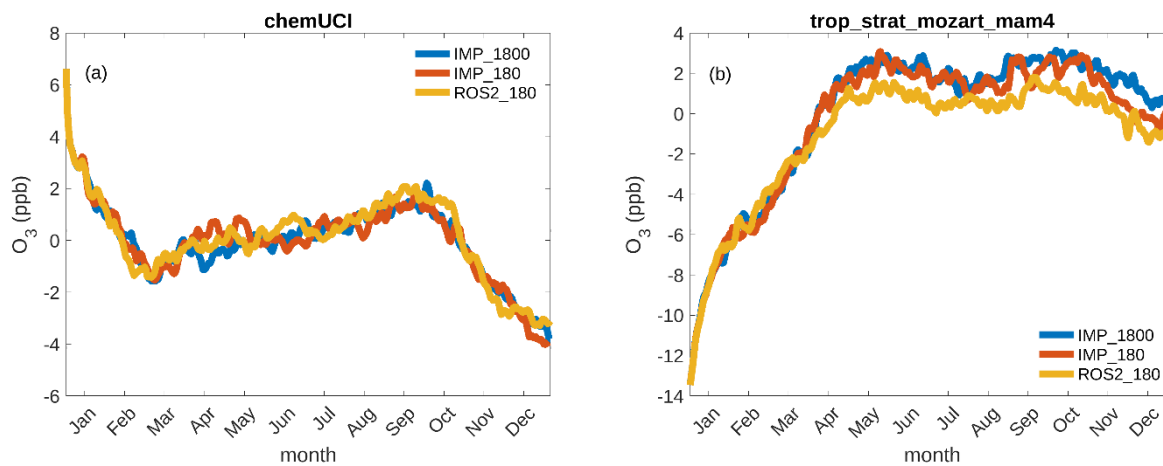
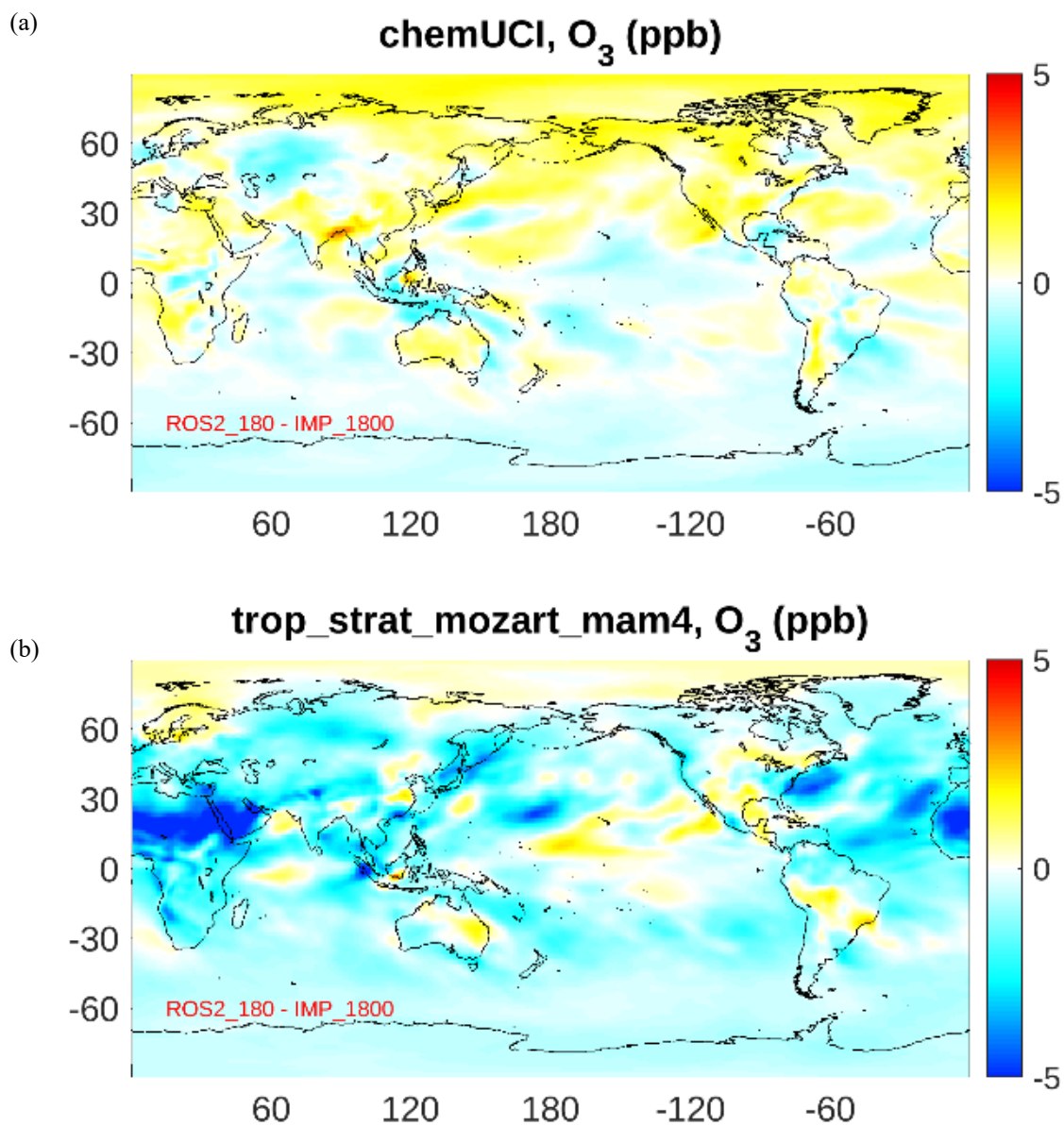


Figure 4. The global daily anomaly of surface ozone compared to the mean of IMP_1800 for (a) chemUCI and (b) trop_strat_mozart_mam4. The blue line is the implicit solver with 1800s as a timestep; the red line is the implicit solver with a timestep of 180s; and the dark yellow line is the Rosenbrock solver with 180s as a time step.



350 Figure 5. The global surface ozone difference between ROS2_180 and IMP_1800 for (a) chemUCI and (b) trop_strat_mozart_mam4.

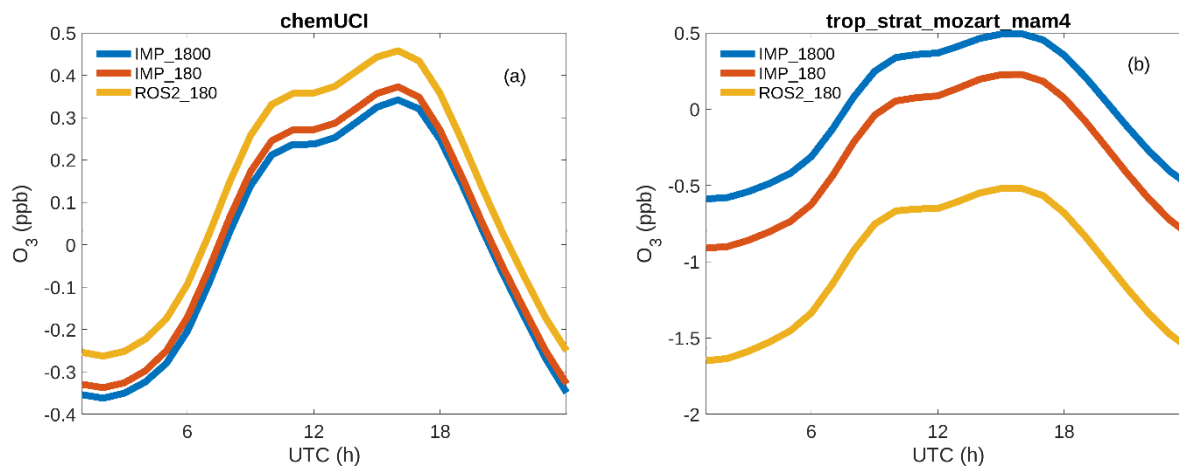


Figure 6. The diurnal cycle for the global surface layer ozone for (a) chemUCI and (b) trop_strat_mozart_mam4. The blue line
355 is the implicit solver with timestep 1800s; the red line is the implicit solver with timestep 180s, and the dark yellow line is the
Rosenbrock solver with timestep 180s.

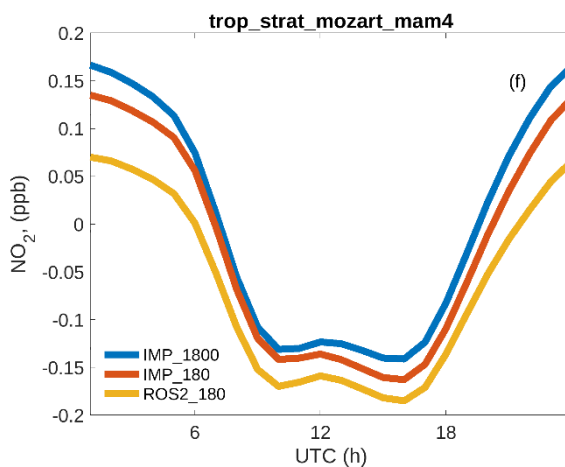
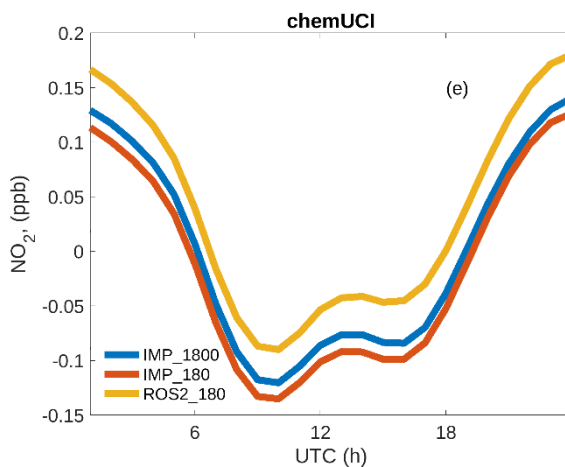
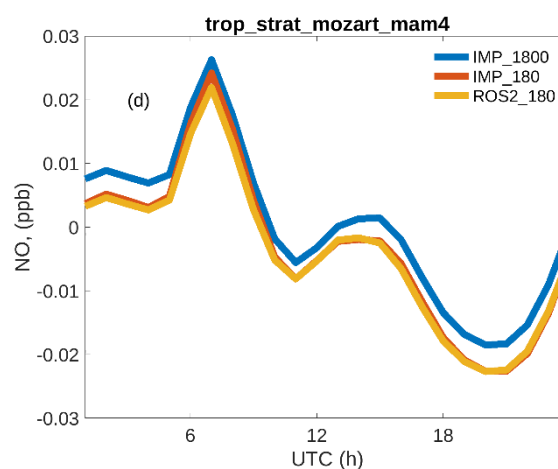
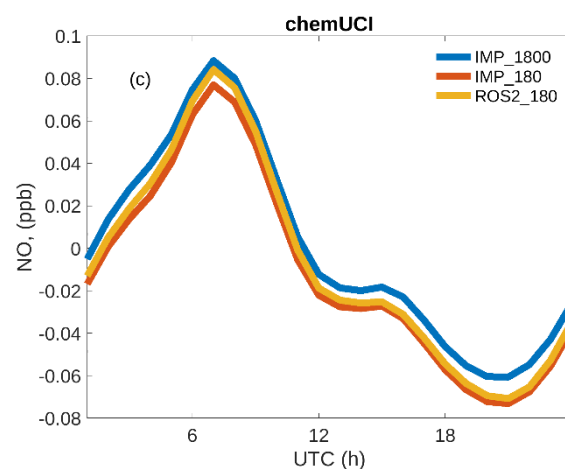
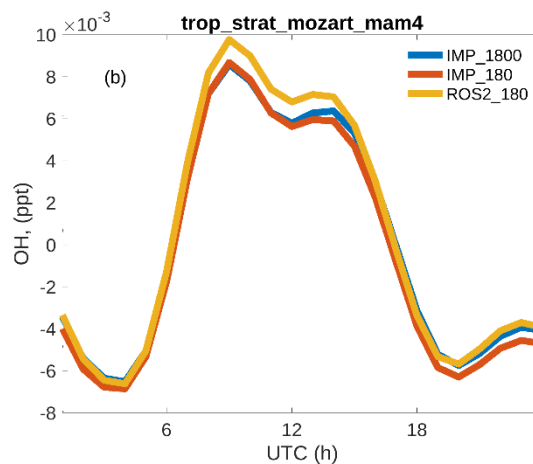
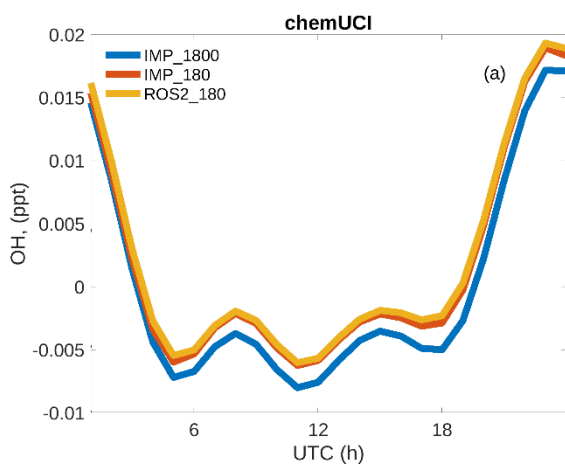




Figure 7. The diurnal cycle of (a) OH, (c) NO, and (e) NO₂ by using chemUCI, (b) OH, (d) NO, and (f) NO₂ by using trop_strat_mozart_mam4. The blue line is the implicit solver with 1800s as timestep; the red line is the implicit solver with 180s as timestep, and the dark yellow is the Rosenbrock solver with 180s as timestep.

365

Code & Data Availability

The E3SM model (Golaz et al., 2019) can be obtained from the E3SM main site. The chemUCI is under the branch tangq/atm/UCI-chem_Jan2021 (Doe) (last access: 2026/03/20), and the trop_strat_mozart_mam4 is under the branch tangq/atm/trop_strat_mam4_resus_mom (Doe) (last access: 2026/03/20). These two branches have been archived under
370 (<https://zenodo.org/records/19745988>) (Tang et al., 2026) (last access: 2026/04/25). The Box model used for testing the convergence rate for this paper can be found in <https://zenodo.org/records/19597033> (Chien and Fu, 2026a) (last access: 2026/04/15), and the input files for the box model can be found in <https://zenodo.org/records/19753716> (Chien and Fu, 2026e) (last access: 2026/04/25). The numerical scheme modules used for this paper and the ROS2 (two-stage Rosenbrock) code can be found in <https://zenodo.org/records/19124522> (Chien and Fu, 2026b) (last access: 2026/03/20). The one-year hourly output
375 for this paper can be found in <https://zenodo.org/records/19703404> (Chien and Fu, 2026d) for chemUCI (last access: 2026/04/25), and in <https://zenodo.org/records/19703406> (Chien and Fu, 2026c) for trop_strat_mozart_mam4 (last access: 2026/04/25).

Author contributions

Conceptualization, Software, Formal analysis, Visualization, and Writing (original draft preparation) RC; Funding acquisition,
380 Supervision, Writing (review and editing) JF.

Disclaimer

Copernicus Publications remains neutral with regard to jurisdictional claims made in the text, published maps, institutional
385 affiliations, or any other geographical representation in this paper. While Copernicus Publications makes every effort to include appropriate place names, the final responsibility lies with the authors. Views expressed in the text are those of the authors and do not necessarily reflect the views of the publisher.



Acknowledgements

This research was supported by a university subproject of the DOE E3SM Project, A Fast Chemistry Solver for E3SM, under
390 Subcontract No. B635004 from Prime Contract No. DE-AC52-07NA27344 through Lawrence Livermore National Laboratory,
funded by the U.S. Department of Energy. This work also used resources of the National Energy Research Scientific
Computing Center (NERSC) under Contract No. DE-AC02-05CH11231 and the Oak Ridge Leadership Computing Facility at
Oak Ridge National Laboratory under Contract No. DE-AC05-00OR22725, both supported by the Office of Science of the
U.S. Department of Energy.

395 Financial support

DOE E3SM Project, A Fast Chemistry Solver for E3SM, under Subcontract No. B635004 from Prime Contract No. DE-AC52-
07NA27344 through Lawrence Livermore National Laboratory, funded by the U.S. Department of Energy.
National Energy Research Scientific Computing Center (NERSC) under Contract No. DE-AC02-05CH11231 and the Oak
Ridge Leadership Computing Facility at Oak Ridge National Laboratory under Contract No. DE-AC05-00OR22725, both
400 supported by the Office of Science of the U.S. Department of Energy.

References

- Brasseur, G. P., Orlando, J. J., and Tyndall, G. S.: Atmospheric Chemistry and Global Change, Topics in environmental
chemistry, Oxford University Press, New York 1999.
- 405 Cariolle, D. and Déqué, M.: Southern hemisphere medium-scale waves and total ozone disturbances in a spectral general
circulation model, *Journal of Geophysical Research*, 91, 10825, 10.1029/jd091id10p10825, 1986.
- Cariolle, D. and Teyssède, H.: A revised linear ozone photochemistry parameterization for use in transport and general
circulation models: multi-annual simulations, *Atmospheric Chemistry and Physics*, 7, 2183-2196, 10.5194/acp-7-2183-2007,
2007.
- 410 Chien, R.-Y. and Fu, J. S.: pshchien/E3SM_ROS2_BOX: ROS2-E3SM Box Model v1.0 for GMD submission (v1.0), Zenodo
[code], 10.5281/zenodo.19597033, 2026a.
- Chien, R.-Y. and Fu, J. S.: pshchien/ROS2-E3SM: ROS2-E3SM v1.1 for GMD submission (v1.1), Zenodo [code],
10.5281/zenodo.19124522, 2026b.
- Chien, R.-Y. and Fu, J. S.: trop_strat_mozart output of the E3SMv1 for GMD submission [dataset],
<https://zenodo.org/records/19703406>, 2026c.
- 415 Chien, R.-Y. and Fu, J. S.: chemUCI output of the E3SMv1 for GMD submission [dataset],
<https://zenodo.org/records/19703404>, 2026d.
- Chien, R.-Y. and Fu, J. S.: Input files for ROS2-E3SM Box Model v1.0 for GMD submission [dataset],
<https://zenodo.org/records/19753716>, 2026e.
- 420 Cionni, I., Eyring, V., Lamarque, J. F., Randel, W. J., Stevenson, D. S., Wu, F., Bodeker, G. E., Shepherd, T. G., Shindell, D.
T., and Waugh, D. W.: Ozone database in support of CMIP5 simulations: results and corresponding radiative forcing,
Atmospheric Chemistry and Physics, 11, 11267-11292, 10.5194/acp-11-11267-2011, 2011.
- E3SMv1 with branch tangq/atm/trop_strat_mam4_resus_mom: [https://github.com/E3SM-
Project/E3SM/tree/tangq/atm/trop_strat_mam4_resus_mom](https://github.com/E3SM-Project/E3SM/tree/tangq/atm/trop_strat_mam4_resus_mom), last access: 2026/03/20.
- 425 E3SMv1 with branch tangq/atm/UCI-chem_Jan2021: [https://github.com/E3SM-Project/E3SM/tree/tangq/atm/UCI-
chem_Jan2021](https://github.com/E3SM-Project/E3SM/tree/tangq/atm/UCI-chem_Jan2021), last access: 2026/03/20.



- Doerfler, D., Austin, B., Cook, B., Deslippe, J., Kandalla, K., and Mendygral, P.: Evaluating the networking characteristics of the Cray XC-40 Intel Knights Landing-based Cori supercomputer at NERSC, *Concurrency and Computation: Practice and Experience*, 30, e4297, 10.1002/cpe.4297, 2018.
- 430 Dunne, J. P., Hewitt, H. T., Arblaster, J. M., Bonou, F., Boucher, O., Cavazos, T., Dingley, B., Durack, P. J., Hassler, B., Jukes, M., Miyakawa, T., Mizielinski, M., Naik, V., Nicholls, Z., O'Rourke, E., Pincus, R., Sanderson, B. M., Simpson, I. R., and Taylor, K. E.: An evolving Coupled Model Intercomparison Project phase 7 (CMIP7) and Fast Track in support of future climate assessment, *Geoscientific Model Development*, 18, 6671-6700, 10.5194/gmd-18-6671-2025, 2025.
- 435 Emmons, L. K., Walters, S., Hess, P. G., Lamarque, J.-F., Pfister, G. G., Fillmore, D., Granier, C., Guenther, A., Kinnison, D., Laepple, T., Orlando, J., Tie, X., Tyndall, G., Wiedinmyer, C., Baughcum, S. L., and Kloster, S.: Description and evaluation of the Model for Ozone and Related chemical Tracers, version 4 (MOZART-4), *Geoscientific Model Development*, 3, 43-67, 10.5194/gmd-3-43-2010, 2010.
- Ferziger, J. H. and Perić, M.: *Computational Methods for Fluid Dynamics*, third, rev. edition., Springer Berlin Heidelberg, Berlin, Heidelberg, 10.1007/978-3-642-56026-2, 2002.
- 440 Golaz, J. C., Caldwell, P. M., Van Roekel, L. P., Petersen, M. R., Tang, Q., Wolfe, J. D., Abeshu, G., Anantharaj, V., Asay-Davis, X. S., Bader, D. C., Baldwin, S. A., Bisht, G., Bogenschutz, P. A., Branstetter, M., Brunke, M. A., Brus, S. R., Burrows, S. M., Cameron-Smith, P. J., Donahue, A. S., Deakin, M., Easter, R. C., Evans, K. J., Feng, Y., Flanner, M., Foucar, J. G., Fyke, J. G., Griffin, B. M., Hannay, C., Harrop, B. E., Hoffman, M. J., Hunke, E. C., Jacob, R. L., Jacobsen, D. W., Jeffery, N., Jones, P. W., Keen, N. D., Klein, S. A., Larson, V. E., Leung, L. R., Li, H. Y., Lin, W., Lipscomb, W. H., Ma, P. L., Mahajan, S., Maltrud, M. E., Mametjanov, A., Mcclean, J. L., Mccoy, R. B., Neale, R. B., Price, S. F., Qian, Y., Rasch, P. J.,
- 445 Reeves Eyre, J. E. J., Riley, W. J., Ringler, T. D., Roberts, A. F., Roesler, E. L., Salinger, A. G., Shaheen, Z., Shi, X., Singh, B., Tang, J., Taylor, M. A., Thornton, P. E., Turner, A. K., Veneziani, M., Wan, H., Wang, H., Wang, S., Williams, D. N., Wolfram, P. J., Worley, P. H., Xie, S., Yang, Y., Yoon, J. H., Zelinka, M. D., Zender, C. S., Zeng, X., Zhang, C., Zhang, K., Zhang, Y., Zheng, X., Zhou, T., and Zhu, Q.: The DOE E3SM Coupled Model Version 1: Overview and Evaluation at Standard Resolution, *Journal of Advances in Modeling Earth Systems*, 11, 2089-2129, 10.1029/2018ms001603, 2019.
- 450 Hauglustaine, D. A., Hourdin, F., Jourdain, L., Filiberti, M. A., Walters, S., Lamarque, J. F., and Holland, E. A.: Interactive chemistry in the Laboratoire de Météorologie Dynamique general circulation model: Description and background tropospheric chemistry evaluation, *Journal of Geophysical Research: Atmospheres*, 109, n/a-n/a, 10.1029/2003jd003957, 2004.
- Hurrell, J. W., Holland, M. M., Gent, P. R., Ghan, S., Kay, J. E., Kushner, P. J., Lamarque, J.-F., Large, W. G., Lawrence, D., Lindsay, K., Lipscomb, W. H., Long, M. C., Mahowald, N., Marsh, D. R., Neale, R. B., Rasch, P., Vavrus, S., Vertenstein, M., Bader, D., Collins, W. D., Hack, J. J., Kiehl, J., and Marshall, S.: The Community Earth System Model: A Framework for Collaborative Research, *Bulletin of the American Meteorological Society*, 94, 1339-1360, 10.1175/bams-d-12-00121.1, 2013.
- 455 Lamarque, J.-F., Emmons, L. K., Hess, P. G., Kinnison, D. E., Tilmes, S., Vitt, F., Heald, C. L., Holland, E. A., Lauritzen, P. H., Neu, J., Orlando, J. J., Rasch, P. J., and Tyndall, G. K.: CAM-chem: description and evaluation of interactive atmospheric chemistry in the Community Earth System Model, *Geoscientific Model Development*, 5, 369-411, 10.5194/gmd-5-369-2012, 2012.
- 460 Lamarque, J.-F., Bond, T. C., Eyring, V., Granier, C., Heil, A., Klimont, Z., Lee, D., Liousse, C., Mieville, A., Owen, B., Schultz, M. G., Shindell, D., Smith, S. J., Stehfest, E., Van Aardenne, J., Cooper, O. R., Kainuma, M., Mahowald, N., McConnell, J. R., Naik, V., Riahi, K., and Van Vuuren, D. P.: Historical (1850–2000) gridded anthropogenic and biomass burning emissions of reactive gases and aerosols: methodology and application, *Atmospheric Chemistry and Physics*, 10, 7017-7039, 10.5194/acp-10-7017-2010, 2010.
- 465 Lamarque, J.-F., Shindell, D. T., Josse, B., Young, P. J., Cionni, I., Eyring, V., Bergmann, D., Cameron-Smith, P., Collins, W. J., Doherty, R., Dalsoren, S., Faluvegi, G., Folberth, G., Ghan, S. J., Horowitz, L. W., Lee, Y. H., Mackenzie, I. A., Nagashima, T., Naik, V., Plummer, D., Righi, M., Rumbold, S. T., Schulz, M., Skeie, R. B., Stevenson, D. S., Strode, S., Sudo, K., Szopa, S., Voulgarakis, A., and Zeng, G.: The Atmospheric Chemistry and Climate Model Intercomparison Project (ACCMIP): overview and description of models, simulations and climate diagnostics, *Geoscientific Model Development*, 6, 179-206, 10.5194/gmd-6-179-2013, 2013.
- 470 Leung, L. R., Bader, D. C., Taylor, M. A., and Mccoy, R. B.: An Introduction to the E3SM Special Collection: Goals, Science Drivers, Development, and Analysis, *Journal of Advances in Modeling Earth Systems*, 12, 10.1029/2019ms001821, 2020.



- 475 Markandya, A., Sampedro, J., Smith, S. J., Van Dingenen, R., Pizarro-Irizar, C., Arto, I., and González-Eguino, M.: Health co-benefits from air pollution and mitigation costs of the Paris Agreement: a modelling study, *The Lancet Planetary Health*, 2, e126-e133, 10.1016/s2542-5196(18)30029-9, 2018.
- Mclinden, C. A., Olsen, S. C., Hannegan, B., Wild, O., Prather, M. J., and Sundet, J.: Stratospheric ozone in 3-D models: A simple chemistry and the cross-tropopause flux, *Journal of Geophysical Research: Atmospheres*, 105, 14653-14665, 10.1029/2000jd900124, 2000.
- 480 McPartland, M. Y., Lovato, T., Koven, C. D., Wilson, J. D., Turner, B., Petrik, C. M., Licón-Saláiz, J., Li, F., Lhardy, F., Clement Kinney, J., Kawamiya, M., Hassler, B., Gillett, N. P., Fall, C. M. N., Danek, C., Brierley, C. M., Bastos, A., and Andrews, O.: CMIP7 Data Request: Earth System Priorities and Opportunities, 10.5194/egusphere-2025-3246, 2025.
- Meinshausen, M., Smith, S. J., Calvin, K., Daniel, J. S., Kainuma, M. L. T., Lamarque, J.-F., Matsumoto, K., Montzka, S. A., Raper, S. C. B., Riahi, K., Thomson, A., Velders, G. J. M., and Van Vuuren, D. P. P.: The RCP greenhouse gas concentrations and their extensions from 1765 to 2300, *Climatic Change*, 109, 213-241, 10.1007/s10584-011-0156-z, 2011.
- 485 Moin, P.: *Fundamentals of Engineering Numerical Analysis*, 1-241 pp., 10.1017/CBO9780511781438, 2010.
- Neale, R. B., Gettelman, A., Park, S., Chen, C.-C., Lauritzen, P. H., Williamson, D. L., Conley, A. J., Kinnison, D., Marsh, D., Smith, A. K., Vitt, F. M., Garcia, R., Lamarque, J.-F., Mills, M. J., Tilmes, S., Morrison, H., Cameron-Smith, P., Collins, W. D., Iacono, M. J., Easter, R. C., Liu, X., Ghan, S. J., Rasch, P. J., and Taylor, M. A.: Description of the NCAR Community Atmosphere Model (CAM 5.0), 10.5065/wgtk-4g06, 2012.
- 490 Prather, M. J. and Zhu, X.: Lifetimes and timescales of tropospheric ozone, *Elem Sci Anth*, 12, 10.1525/elementa.2023.00112, 2024.
- Prather, M. J., Zhu, X., Flynn, C. M., Strode, S. A., Rodriguez, J. M., Steenrod, S. D., Liu, J., Lamarque, J.-F., Fiore, A. M., Horowitz, L. W., Mao, J., Murray, L. T., Shindell, D. T., and Wofsy, S. C.: Global atmospheric chemistry – which air matters, *Atmospheric Chemistry and Physics*, 17, 9081-9102, 10.5194/acp-17-9081-2017, 2017.
- 495 Rosenbrock, H. H.: Some general implicit processes for the numerical solution of differential equations, *The Computer Journal*, 5, 329-330, 10.1093/comjnl/5.4.329, 1963.
- Sandu, A., Verwer, J. G., Blom, J. G., Spee, E. J., Carmichael, G. R., and Potra, F. A.: Benchmarking stiff ode solvers for atmospheric chemistry problems II: Rosenbrock solvers, *Atmospheric Environment*, 31, 3459-3472, 10.1016/s1352-2310(97)83212-8, 1997a.
- 500 Sandu, A., Verwer, J. G., Van Loon, M., Carmichael, G. R., Potra, F. A., Dabdub, D., and Seinfeld, J. H.: Benchmarking stiff ode solvers for atmospheric chemistry problems-I. implicit vs explicit, *Atmospheric Environment*, 31, 3151-3166, 10.1016/s1352-2310(97)00059-9, 1997b.
- Santillana, M., Le Sager, P., Jacob, D. J., and Brenner, M. P.: An adaptive reduction algorithm for efficient chemical calculations in global atmospheric chemistry models, *Atmospheric Environment*, 44, 4426-4431, <https://doi.org/10.1016/j.atmosenv.2010.07.044>, 2010.
- 505 Sun, J., Fu, J. S., Drake, J., Lamarque, J. F., Tilmes, S., and Vitt, F.: Improvement of the prediction of surface ozone concentration over conterminous U.S. by a computationally efficient second-order Rosenbrock solver in CAM4-Chem, *Journal of Advances in Modeling Earth Systems*, 9, 482-500, 10.1002/2016ms000863, 2017.
- 510 Szopa, S., Naik, V., Adhikary, B., Artaxo, P., Berntsen, T., Collins, W. D., Fuzzi, S., Gallardo, L., Kiendler-Scharr, A., Klimont, Z., Liao, H., Unger, N., and Zanis, P.: Short-lived Climate Forcers, in: *Climate Change 2021 – The Physical Science Basis*, Cambridge University Press, 817-922, 10.1017/9781009157896.008, 2023.
- Tang, Q. and Prather, M. J.: Five blind men and the elephant: what can the NASA Aura ozone measurements tell us about stratosphere-troposphere exchange?, *Atmospheric Chemistry and Physics*, 12, 2357-2380, 10.5194/acp-12-2357-2012, 2012.
- 515 Tang, Q., Taylor, M. A., Hsu, J., Prather, M. J., and Wu, M.: E3SMv1 branch used for the GMD submission [code], <https://zenodo.org/records/19745988>, 2026.
- Tilmes, S., Lamarque, J.-F., Emmons, L. K., Kinnison, D. E., Ma, P.-L., Liu, X., Ghan, S., Bardeen, C., Arnold, S., Deeter, M., Vitt, F., Ryerson, T., Elkins, J. W., Moore, F., Spackman, J. R., and Val Martin, M.: Description and evaluation of tropospheric chemistry and aerosols in the Community Earth System Model (CESM1.2), *Geoscientific Model Development*, 8, 1395-1426, 10.5194/gmd-8-1395-2015, 2015.
- 520 Vandyck, T., Keramidas, K., Kitous, A., Spadaro, J. V., Van Dingenen, R., Holland, M., and Saveyn, B.: Air quality co-benefits for human health and agriculture counterbalance costs to meet Paris Agreement pledges, *Nature Communications*, 9, 10.1038/s41467-018-06885-9, 2018.

<https://doi.org/10.5194/egusphere-2026-1451>

Preprint. Discussion started: 28 April 2026

© Author(s) 2026. CC BY 4.0 License.



525 Verwer, J. G., Spee, E. J., Blom, J. G., and Hundsdorfer, W.: A Second-Order Rosenbrock Method Applied to Photochemical Dispersion Problems, *SIAM Journal on Scientific Computing*, 20, 1456-1480, 10.1137/s1064827597326651, 1999.